J Amer Oil Chem Soc (2007) 84:709–716
DOI 10.1007/s11746-007-1092-y

ORIGINAL PAPER

Diminishing Marginal Utility of Cooling Rate Increase on the Crystallization Behavior and Physical Properties of a Lipid Sample

K. L. Humphrey · S. S. Narine

Received: 15 June 2006 / Revised: 19 March 2007 / Accepted: 23 May 2007 / Published online: 11 July 2007

Abstract It is well established that variation of the rate of cooling (*r)* of a lipid sample is an effective tool to influence the crystallization process and effect changes in network structure and physical functionality. However, the extent of the physical changes does not always justify the extent to which the cooling rate must be altered. It is therefore important to understand the rates at which marginal changes in physical functionality begin to diminish, and to understand the mechanisms which introduce such limitations. A commercially available cocoa butter alternative, Temcote (Bunge Oils, Bradley, IL), was crystallized under cooling rates varying from 0.1 to 20 °C min^{-1}. The growth mode and polymorphism of each sample was studied using DSC and X-ray diffraction (XRD). The hardness of the sample was monitored using cone penetrometry and its solid fat content (SFC) evolution was monitored using a temperature controlled pulse-NMR. The data demonstrates that the melting profile of the sample could be greatly manipulated over a relatively narrow range of cooling rates. Large increases in cooling rate increase the final SFC of the sample by approximately 6%. Doubling the cooling rate increases the hardness of the sample 50%. Variation of the cooling rate as a tool to modify physical functionality of the network was found to be effective only for cooling rates lower than 5 °C min^{-1}.

K. L. Humphrey · S. S. Narine (✉)
Alberta Lipid Utilization Program, Department of Agricultural, Food and Nutritional Science, University of Alberta, 4-10 Agricultural/Forestry Centre, Edmonton, AB T6G 2P5, Canada
e-mail: Suresh.narine@ualberta.ca

K. L. Humphrey
e-mail: klh5@ualberta.ca

Keywords Cocoa butter alternatives · Crystal structure · Final physical properties · Growth from melt · Kinetics · *Rates of cooling*

Introduction

Non-isothermal crystallization studies of lipids are of significant interest, particularly for the food industry. The effect of processing conditions, such as cooling rate and degree of supercooling, on the structure and physical properties of crystallizing systems has been investigated by several researchers [1–6]. In this regard, the crystallization behavior of lipids, including cocoa butter and its alternatives, has been given particular attention [7–13]. It has been shown that the cooling rate (r) affects the structural order of a crystallized sample, which in turn influences the final properties of the lipid network. Faster cooling rates during non-isothermal crystallization result in a higher degree of supercooling than slow cooling rates at any point in time (t_1) during the cooling process, as shown in Fig. 1. When a lipid sample is cooled quickly, the system crystallizes before the optimal spatial organization of the molecules is reached due to insufficient mass transfer rates. Conversely, during slower cooling rates, mass transfer rates are increased (due to lower viscosity and longer induction time prior to solidification) and the organization of the molecules occurs faster and to a greater extent [4, 6, 14, 15]. The rate of cooling may cause changes in the growth mode of the network, and can lead to polymorphic, microstructural, and solid fat content changes, and therefore, changes in the final physical properties of the network [16, 17].

Cocoa butter alternatives (CBA) are of significant industrial importance. They are typically less expensive than cocoa butter and generally require much less careful

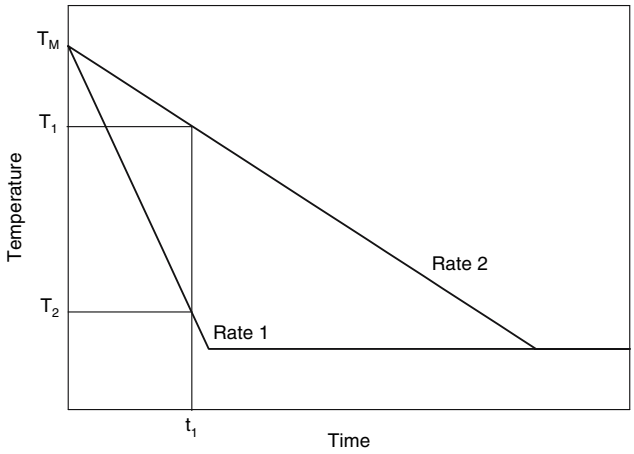

Fig. 1 Effect of rate of cooling on the supercooling of a sample

tempering [9]. CBA can have a longer shelf life, be less afflicted by bloom, and tend to have a bland taste that can be easily masked during the production of confectionary products [9]. Although CBAs do not require the strict tempering regimes which cocoa butter demands, the processing conditions to which they are subjected are of importance to the confectionary industry, particularly from the perspective of influencing physical properties such as hardness.

This paper presents non-isothermal crystallization studies of a CBA, Temcote. It investigates the effect of the rate of cooling on the hardness, polymorphism, induction time, and enthalpies of crystallization and melt of a CBA, Temcote, by supercooling the sample at different rates varying from 0.1 to 20 °C min^{-1}. The range of cooling rates, which produces notable changes to the crystallization process was particularly examined. The final physical properties of the samples were determined and discussed.

Experimental Procedures

The lipid sample used in this study was Temcote, a CBA supplied by Bunge Oils (Bradley IL, USA). Unaltered Temcote, with a melting point of 34.7 ± 0.2 °C (when crystallized at 10 °C min^{-1} and melted at 5 °C min^{-1}), was used for all measurements. The rates of cooling for the NMR and hardness measurements were determined using a soybean oil sample, which does not crystallize in the temperature range used. Sample cooling and heating rates are reported to a certainty of ± 0.1 °C min^{-1}. The static measurements were performed at a stage temperature of 15.0 ± 0.5 °C. The samples were stored in a cooling chamber at 15.0 ± 0.5 °C. All measurements were performed in triplicate (n = 3) and the mean values are reported with their subsequent standard deviations.

Sample Preparation

The sample was heated to 90 °C and stirred with a mechanical stirrer for 2 min to ensure homogeneity and to destroy crystal memory and then transferred to the appropriate container (aluminum pans for DSC, brass compression mold for hardness and appropriate tubes for NMR and XRD) for analysis. The sample was equilibrated at 90 °C for 5 min and then cooled at a prescribed constant rate, ranging from 0.1 to 20 °C min^{-1}, down to a holding temperature of 15 °C.

Cone Penetrometry, Hardness Measurements

The molten fat was transferred into a brass compression mold to make sample disks of 2.4 ± 0.1 cm in diameter and 0.3 ± 0.1 cm thick. The brass mold containing the Temcote was then sealed and waterproofed. The Temcote samples were processed in the mold inside a water bath. The samples were cooled from 90 to 15 °C at 13 different cooling rates (0.1, 0.5, 1, 2, 3, 4, 5, 6, 7, 8, 9, 10, and 20 °C min^{-1}). After thermal processing, the samples were stored for 24 h at 15 °C, and subsequently removed from the mold prior to measurements.

The "Precision Penetrometer" from Precision Scientific Company, Chicago, USA was used to measure the hardness. It was fitted with a stainless steel penetration cone of mass 45.0 ± 0.5 g and angle of 22.5°. The hardness is related to the distance into which the cone penetrates the sample over a 5 s time period. The displacement of the cone was read on the Vernier scale on the instrument in 1/10 mm.

DSC Measurements, Thermal Behavior

A "DSC 2920 Modulated DSC" by TA Instruments was used in the non-modulated DSC mode for thermal measurements. Liquid Temcote was pipetted in consistent amounts (10–15 mg each) into three aluminum DSC pans, which were then hermetically sealed. An empty aluminum pan was used as a reference. The samples were first equilibrated at 90 °C for 5 min and then cooled at the prescribed rate (0.1, 0.5, 1, 2, 3, 4, 5, 6, 7, 8, 9, 10, 11, 12, 13, 14, 15, 16, 17, 18, 19, and 20 °C min^{-1}) down to –10 °C where they were equilibrated for 15 min to allow crystallization to complete. The sample was then heated to 90 °C at a constant rate of 5 °C min^{-1} to obtain the melting curve.

The data sampling and temperature control procedures were fully automated and controlled by the "TA Instrument Control" software program. The data was analyzed using the "TA Universal Analysis" software and a method developed by our group [18]. All curves were normalized to a uniform sample mass of 15 mg.

XRD Measurements, Polymorphism

A "Bruker AXS X-ray diffractometer" equipped with a filtered Cu-Kα radiation source (λ = 0.1542 nm) was used for XRD analysis. The procedure was automated and commanded by Bruker AXS' "General Area Detector Diffraction System" (GADDs V 4.1.08) software. The XRD samples were prepared by filling glass capillary tubes with the molten sample. The tubes were fitted with the brass sample holder and then tempered at a prescribed rate (0.1, 1, … to 20 °C min^{-1}) down to the final holding temperature of 15 °C in a "Linkam LTS 350" temperature controlled stage (Linkam Scientific Instruments, Tadworth, Surrey, United Kingdom) using its "Air Jet" cooling system (Kinetics-Thermal Systems, New York, USA). The sample was held isothermally in the Linkam for 30 min at this final temperature. The sample tube with brass holder was then quickly transferred for analysis to the XRD stage. The XRD frames, obtained after 450 s exposure to a monochromatic Cu-Kα X-ray beam, were processed using GADDS software and the resulting spectra were analyzed using Bruker AXS's "Topas V 2.1" software.

NMR Measurements, SFC Determination

SFC data was acquired using the pulse magnetic resonance spectrometer "minispec mq SFC analyzer" (Bruker Instruments, Milton, Ontario, Canada), equipped with a temperature controlled measurement chamber. SFC sampling as a function of time and temperature was accomplished using a custom-designed cooling system previously described [19]. The data sampling procedure was fully automated, and the SFC was calculated and displayed by the "minispec v2.20 Rev.01/NT" software.

The NMR tubes were filled with molten fat to a height of 3.5 ± 0.1 cm. To achieve the prescribed cooling rate, the samples were first heated to 90 °C and held there for 5 min before being cooled from 90 to 67 °C outside of the NMR apparatus using external water baths and then transferred rapidly into the NMR chamber and cooled from 67 to 15 °C inside the NMR chamber. The sample was then held isothermally inside the NMR chamber for 24 h at 15 °C. Twelve cooling rates (0.1, 0.5, 0.9, 1.6, 3.0, 3.5, 4.3, 5.2, 7.7, 10.2, 12.5, and 15.9 °C min^{-1}) were used. The SFC was measured at 10 s intervals starting the instant the sample was introduced into the NMR chamber. The plateau portion of the SFC curve was determined unambiguously by using the first and second derivatives of the SFC versus time curve. The starting point of the plateau was taken to be the initial point of the constant portion of the first derivative and the zero of the second derivative. The first derivative was considered constant if its value was within three times the peak to peak (ptp) noise of its average. A portion of the curve is considered constant if the SFC values over the interval were within two times the ptp noise level of the average SFC value of the interval. The value for a linear portion of the second derivative of zero was used accordingly. The reported final SFC value is the average of the experimental plateau portion of the curve.

Results and Discussion

Figure 2 shows the hardness of the samples measured by cone penetrometry as a function of *r*. As the rate of cooling increases, the penetration distance decreases smoothly and rapidly from 1.70 ± 0.08 mm for the sample cooled at 0.1 °C min^{-1} to plateau at about 1.01 ± 0.01 mm, a hardness value first achieved by the sample processed at 3.0 °C min^{-1}. This represents an increase in hardness of 68.3% over a 30-time increase in cooling rate. Interestingly, there is a 50% increase in hardness as the cooling rate increases by a factor of six from 0.5 to 3.0 °C min^{-1}. Clearly, the range of cooling rates over which the hardness of this sample is significantly affected is very small. Therefore, the data indicates that cooling tunnels through which this lipid sample is processed should be carefully regulated, as small changes in rate can potentially cause large changes in hardness. Furthermore, the data indicates that for this particular sample, slow cooling rates are sufficient to produce maximum hardness. Deviations from the increasing hardness trend at 4, 5, and 10 °C min^{-1} cooling rates are not significant enough to warrant an alternate explanation as the general trend in within error bars. Additionally, given the error spread in the data, the hardness at these rates are for all practical purposes within the plateau region.

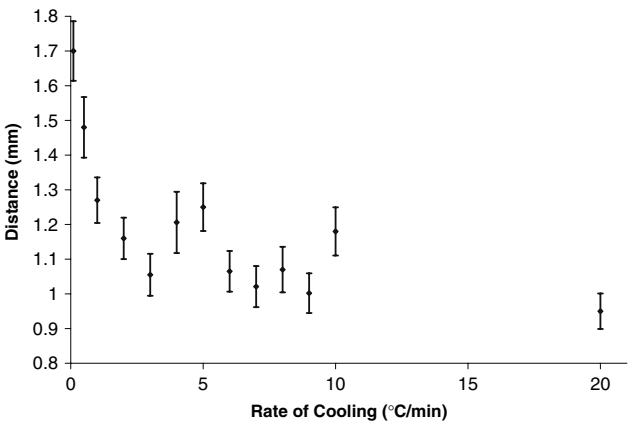

Fig. 2 Hardness by cone penetrometry versus cooling rate

Figure 3 shows the crystallization curves for all rates versus time with the curve for the sample cooled at 0.1 °C min^{-1} being the bottom line each subsequent curve representing samples cooled at progressively faster rates of cooling with the 20 °C min^{-1} rate being the uppermost curve on the graph. The sample demonstrated relatively homogeneous crystallization behavior. The DSC crystallization curves (Fig. 3) show a main broad peak (arrow 1) proceeded by a shoulder (arrow 2) measurable for all cooling rates. As r is increased, the shoulder peak became increasingly more prominent suggesting the promotion of a growing discrimination in the crystallization of two fractions representative of differentiated molecular ensembles of the CBA. The onset of crystallization (T_o) and the start of crystallization (T_s) shown in Fig. 4a, the maximum crystallization temperature (T_{max}) and the position of the inflection point of the shoulder shown in Fig. 4b decrease almost linearly as the cooling rate increases from r = 1 to 12 °C min^{-1} and then plateau for higher cooling rates. The onset of crystallization was taken as the point of intercept

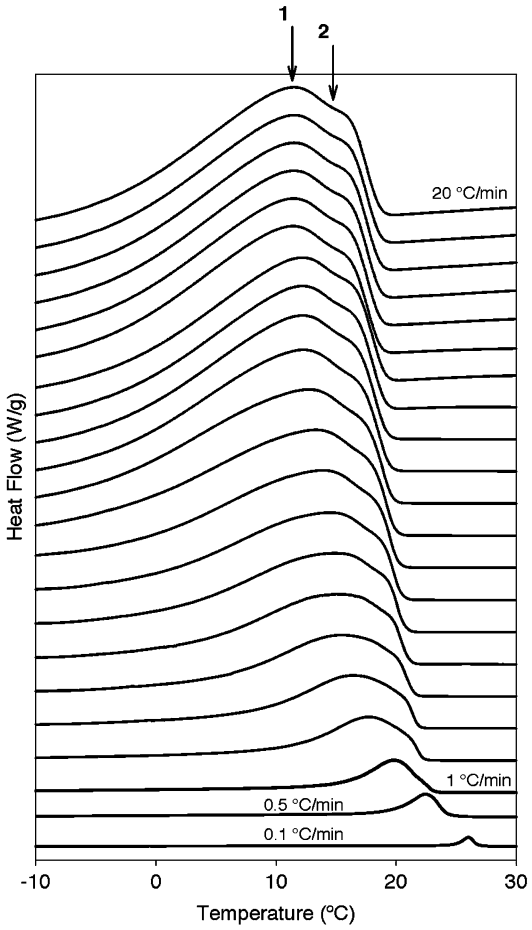

Fig. 3 Stacked crystallization curves for samples processed at all cooling rates from 0.1 °C min^{-1} (*bottom line*) to 20 °C min^{-1} (*uppermost line*)

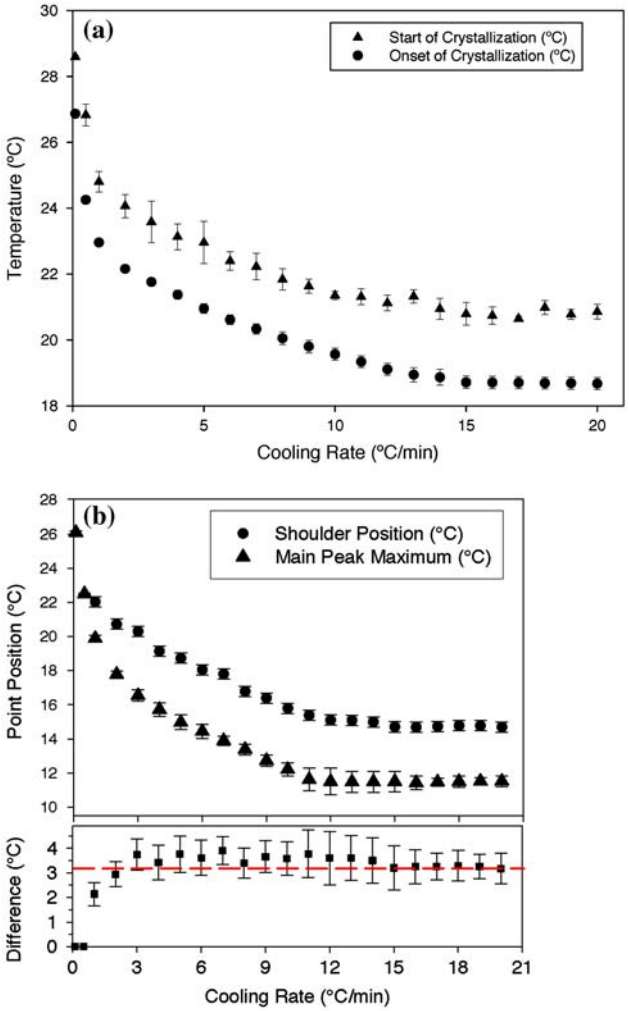

Fig. 4 **a** Onset of crystallization and start of crystallization event versus cooling rate. **b** Location of peak maximum and shoulder peak of the crystallization event versus cooling rate

of the tangent on the steepest slope of the peak to the baseline of the signal and the start of crystallization (T_s) was chosen as the point at which the heat flow signal first deviates from the baseline. It is interesting to note that the effective increase in super cooling due to increases in cooling rate has the effect of depressing the onset of crystallization. The most likely explanation for this is that the rate of increase of viscosity is high due to the faster rate of cooling, that mass transfer becomes a limiting factor in crystallization. This effect has been noted, if not explained, by others before [15].

With the final crystallization temperature not much removed from the melting temperature, if one compares low cooling rates to high cooling rates of the same lipid ensemble, regardless of the speed of the temperature decrease, at the point that the crystallization temperature is achieved, the effective super cooling is relatively the same. Super cooling is dependent on the difference of (T_M–T_C),

where T_M is the melting temperature (or beginning of melt for a complex sample) and T_C is the crystallization temperature. Therefore, if T_M–T_C is small, regardless of the speed at which this difference is achieved, the super cooling remains relatively unchanged. However, the rate of cooling in such circumstances does have a significant impact on the rate of viscosity increase. Liquid lipid samples demonstrate an exponential increase in viscosity as temperature is decreased as shown in Fig. 5 for Temcote. Therefore, if the crystallization temperature is sufficiently high, as it was in this experiment with the onset of melt (16 ± 1 °C) being very close to the final crystallization temperature (15.0 ± 0.5 °C), one would have increased the viscosity (and therefore, decreased the mass transfer of molecules in the melt) faster due to an increased cooling rate while providing a relatively small increase in thermodynamic driving force. Under such conditions it will take longer for mass transfer to occur prior to crystallization, resulting in a depression of the onset of crystallization. The extent to which the inception of crystallization, of molecular ensembles differentiated by radius of gyration and complexity of the molecule itself would be affected by such limitations to mass transfer, would provide the basis for the behavior demonstrated by the CBA sample in this experiment. Therefore, fractionation is possible by preferentially retarding the mass transfer of specific families of TAGs, hereby permitting some to crystallize earlier. Of course, it is expected that some limiting viscosity would be reached, at which point the differentiation and depression of onset of crystallization due to mass transfer limitations would no longer be relevant as demonstrated by plateau region shown in Fig. 4a. This is also in keeping with the exponential nature of the viscosity relationship with temperature (there is a plateau region). T_o decreases smoothly with increasing cooling rate from 22.9 ± 0.1 °C for r = 1 °C min^{-1}, and plateaus at 19.0 ± 0.3 °C for rates above 12 °C min^{-1}. T_s decrease similarly with an average difference in temperature (T_s–T_o) of 1.8 ± 0.1 °C. The temperature difference between the main peak and the shoulder is practically constant (3.5 ± 0.2 °C) for cooling rates higher than 5 °C min^{-1} indicating that the ensemble crystallizes homogeneously one before the other regardless of the magnitude of the cooling rate and that there is no thermal influence of one ensemble on the other. Therefore, at rates higher than 5 °C min^{-1}, the retardation effect of one fraction of molecules versus the other seems to be equally effective. The gap between the two events narrows when r is decreased below 5 °C min^{-1}. It would therefore seem that at these rates, the mass transfer limitations due to viscosity are less effective for one fraction versus the other. It is uncertain as yet how this behavior translates to the macro scale so that it affects hardness. It is worth noting that the hardness is also affected within the range where there is a discriminatory effect of the viscosity limitations to mass transfer of one fraction of molecules versus the other within the sample. Note also that the evolution of the crystallization event's main peak and shoulder heights mirror that of the respective positions. The heights increase in a linear fashion from r = 1 to 12 °C min^{-1} and then plateau for higher cooling rates.

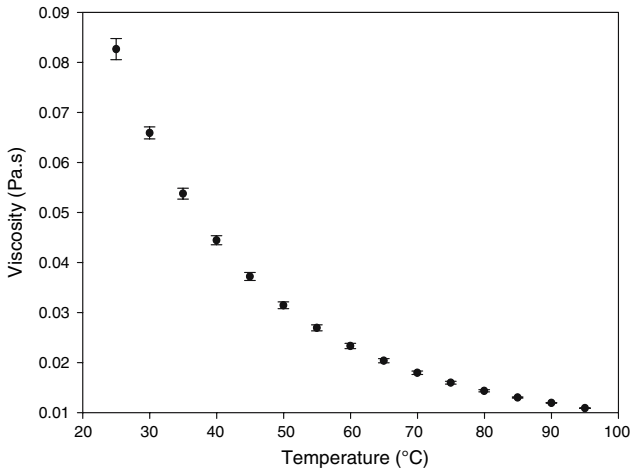

Fig. 5 Viscosity of Temcote as a function of temperature

Figure 6 shows the melting curves of the sample for all cooling rates. The lowermost line is the melting curve for the sample cooled at 20 °C min^{-1}, and subsequently higher curves represent the samples cooled at incrementally slower rates with the uppermost line representing the melting endotherm for the sample cooled at 0.1 °C min^{-1}. The overall time of melting as determined from the start to the end of the event is 10.4 ± 0.2 min for all rates. The melting curves display a small resolved peak (P1) followed by a large main peak (P_{main}) made of overlapping events at the high-end temperature. This complex melting behavior is commonly observed for lipid samples [20]. An extra intermediary minor peak (P2) around 15 °C is displayed in the curves obtained with the three first cooling rates (r = 1, 2 and 3 °C min^{-1}) and shows as a broad shoulder in the curves obtained with r = 4 and 5 °C min^{-1}. P2 becomes incorporated in the main melting event as the main peak broadens. The appearance of such small peaks for samples cooled at slow rates of cooling is well known and is characteristic of the formation of compounds, which would not have the time to grow otherwise. The disappearance of smaller peaks at higher rates of cooling is common and has been previously reported [21].

Due to the overlap of melting peaks, it is only possible to estimate the FWHM of the main melting endotherm by measuring the half width at half maximum starting from the end of the peak (and multiplying by 2). The main melting peak as described by its FWHM is narrow. As

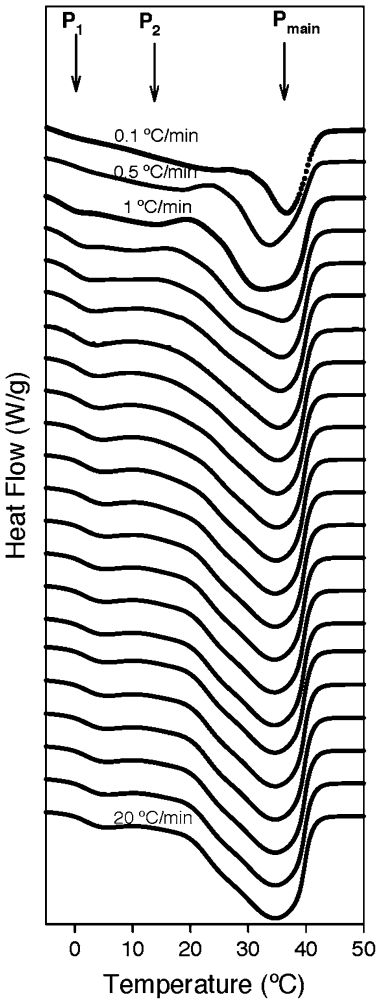

Fig. 6 Stacked melting curves for samples processed at all cooling rates from 1 °C min^{-1} (*uppermost line*) to 20 °C min^{-1} (*bottom line*)

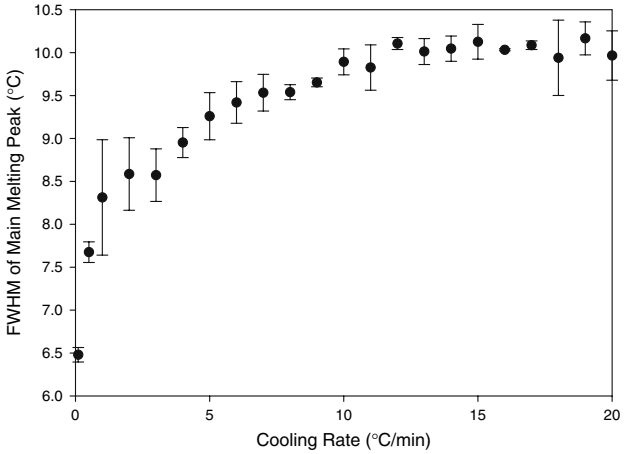

Fig. 7 FWHM of the main melting peak versus cooling rate as a function of temperature

shown in Fig. 7, FWHM increases smoothly with increasing r in an exponential-like manner from 6.5 ± 0.1 °C for the lowest r and plateaus at 10.1 ± 0.1 °C. Ninety five percent of this value has been reached for r = 11 °C min^{-1}. Note that the small variation, less than 2 °C (for samples cooled at rates greater than 1 °C min^{-1}), would not be noticeable by the end consumer upon ingesting the fat product. Such a low FWHM with respect to temperature value combined with similar melting points is indicative of compounds melting catastrophically, leading to a mouth-feel independent of the rate of cooling.

The trend in FWHM of the main melting peak (as described above) matches the evolution of the hardness. It is therefore, reasonable to think that the larger number of compounds formed (indicated by a higher FWHM) greatly influence the evolution of hardness with softer samples having a lower FWHM and thus a greater similarity in the types of compounds formed. Thus crystallization at higher cooling rates (>5 °C min^{-1}) forms compounds, which melt over a wider range of temperatures, which lead to the formation of a harder final product. It is therefore, possible to adjust the physical properties, such as melting and potentially hardness, and extend the range of cooling rates used beyond 4 °C min^{-1} by adjusting the composition of the CBA. The effect of changing the composition of a fat sample to alter its physical properties has been seen before [22–26]. Of course, such a possibility is dependent on the identification of the compounds responsible for the desired physical property.

Typically cocoa butter alternatives do not demonstrate polymorphic behavior. However, the polymorphism of the lipid sample versus cooling rates was investigated for completeness. The d-values (3.85 ± 0.01 and 4.23 ± 0.01 μm) obtained from XRD measurements were practically independent of r and are typical values indicative of the beta-prime polymorphic form. The resolution of our XRD system could not resolve for the different types of beta-prime polymorph and therefore the exact stable phases reached after the thermal treatment were not accessible. Time-resolved XRD analysis must be used to solve for the polymorphic transitions occurring during melting and explain the occurrence of multiple melting peaks observed in the DSC thermogram [20]. However, because the principal polymorphic form of the sample desired for CBA based products is not affected, the cooling rate could be used to adjust parameters such as the onset time and melt temperature to achieve desired physical properties.

Figure 8a shows representative SFC versus time curves for cooling rates of 15.9, 1.6 and 0.1 °C min^{-1}. For the lower cooling rates, the crystallization event consists of at least two cascading events (as is evident for the 0.1 °C min^{-1} SFC curve and indicated by the arrow showing the prominent inflection region) suggesting the

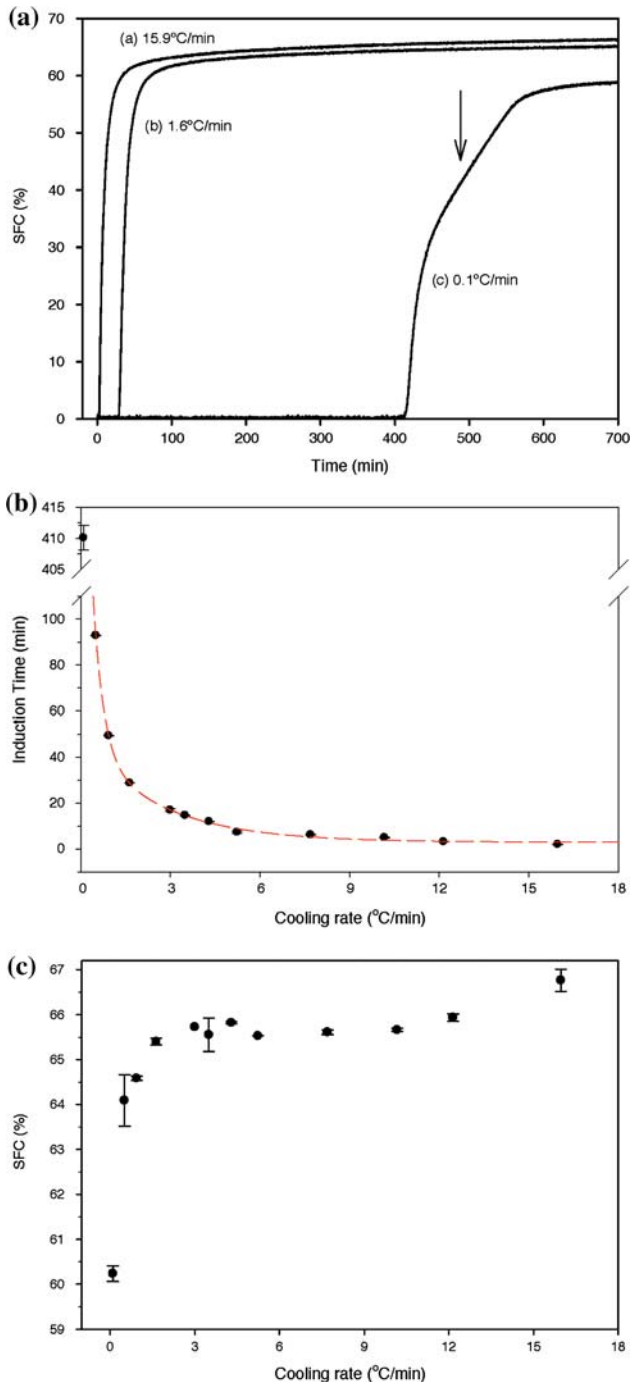

Fig. 8 **a** SFC versus time. From *left to right* curves obtained with 15.9, 1.6, and 0.1 °C min^{-1} cooling rate. **b** Induction time versus cooling rate by NMR. **c** Final SFC versus cooling rate by NMR

occurrence of secondary crystallization. Crystallization occurring over multiple steps in lipid materials has been frequently reported in the literature [13, 18, 27]. The onset time for crystallization, obtained via NMR (Fig. 8b), decreases dramatically as r increases. One would expect longer onset time prior to crystallization due to the increased time for the required supercooling to occur prior to nucleation. However, samples may crystallize at higher temperatures when cooled at slower rates because the increased time at higher temperatures leads to the molecules within the melt having more internal energy allowing for the molecules to move about within the melt and achieve a desired conformation at a higher crystallization temperature. The variations of onset time of crystallization from DSC are similar.

The final SFC of the sample increases by 6% with increasing rate of cooling and plateaus at 65.5 ± 0.4% for a cooling rate of approximately 4 °C min^{-1} as shown in Fig. 8c. Seventy percent of the increase in final SFC occurred for samples cooled with 0.1 and 0.5 °C min^{-1}. This suggests that undercooling conditions were met for most of the components in the melt with cooling rates as small as 0.5 °C min^{-1}. It is interesting to notice that the 5 °C min^{-1} threshold is found again in the SFC characteristics and could further support the trends found in the hardness of the sample cooled at varying rates.

The cooling rate of a cocoa butter alternative can be altered to achieve the desired physical functionality without affecting the polymorphism. Variation of the cooling rate as a tool to modify physical functionality of the network was found to be effective only for cooling rates lower than 5 °C min^{-1}. The data demonstrates that the melting profile of the sample could be manipulated over a relatively narrow range of cooling rates. The thermal characteristics of the main CBA's components could be altered to some extent by varying the cooling rates lower than 12 °C min^{-1}. The components, which are thought to be lower melting components of the CBA could be only affected by cooling rates lower than 5 °C min^{-1}. There is marginal utility to increasing the rate above these values, as there are limitations to the hardness and melting properties which one cocoa butter alternative can have.

Increasing the cooling rate could only be used to increase final SFC by approximately 6%. The variation of the main characteristics versus cooling rate determined by SFC is consistent with DSC data and account for hardness results.

It is therefore, suggested that the effect of cooling rate variation on modification of physical functionality of a lipid sample is effective over limited ranges of cooling rates, determined by the ability for the molecules to move within the melt at high temperatures prior to the crystallization event.

Acknowledgments We would like to thank Bunge Oils, the Alberta Crop Industry Development Fund, the Alberta Agricultural Research Institute, the Alberta Canola Producers Commission and National Sciences and Engineering Research Council for financial support for the research as well as Ereddad Kharraz, Baljit Ghotra, Marc Boodhoo and Sandra Dyal for assistance with sample preparation and data acquisition.

References

1. Akazawa T, Inaguma Y, Katsumata T, Hiraki K, Takahashi T (2004) Flux growth and physical properties of pyrochlore Pb2Ru2O6.5 single crystals. J Cryst Growth 271:445–449
2. Cashell C, Corcoran D, Hodnett BK (2004) Control of polymorphism and crystal size of L-glutamic acid in the absence of additives. J Cryst Growth 273:258–265
3. Herrera M, Falabella C, Melgarejo M, Anon M (1998) Isothermal crystallization of hydrogenated sunflower oil: 1. nucleation. J Am Oil Chem Soc 75:1273–1280
4. Herrera M (1994) Crystallization behavior of hydrogenated sunflower-seed oil: kinetics and polymorphism. J Am Oil Chem Soc 71:1255–1260
5. Herrera M, Segura JA, Rivarola G, Anon M (1992) Relationship between cooling rate and crystallization behavior of hydrogenated sunflower-seed oil. J Am Oil Chem Soc 69:898–905
6. Martini S, Herrera M, Hartel R (2002) Effect of cooling rate on crystallization behavior of milk fat fraction/sunflower oil blends. J Am Oil Chem Soc 79:1055–1062
7. Cebula DJ, Smith KW (1991) Differential scanning calorimetry of confectionery fats. Pure triglycerides: effects of cooling and heating rate variation. J Am Oil Chem Soc 68:591–595
8. Rousset P, Rappaz M (1997) Alpha-melt-mediated crystallization of 1-palmitoyl-2-oleoyl-3-stearoyl-sn-glycerol. J Am Oil Chem Soc 74:693–697
9. Rousset P, Rappaz M (1996) Crystallization kinetics of the pure triacylglycerols glycerol-1, 3-dipalmitate-2-oleate, glycerol-1-palmitate-2-oleate-3-stearate, and glycerol-1, 3-distearate-2-oleate. J Am Oil Chem Soc 73:1051–1057
10. Kerti K (1998) In: 2nd International workshop on control applications in postharvest and processing technology. Sigrimis N, and P Groumpos, (eds) Budapest, Hungary), p. 173–176
11. Metin S, Hartel RW (1996) Crystallization behavior of blends of cocoa butter and milk fat or milk fat fractions. J Therm Anal 47:1527–1544
12. Metin S, Hartel R (1998) Thermal analysis of isothermal crystallization kinetics in blends of cocoa butter with milk Fat or milk fat fractions. J Am Oil Chem Soc 75:1617–1624
13. Perez-Martinez D, Alvarez-Salas C, Morales-Rueda J, Toro-Vazquez J, Charo-Alonso M, Dibildox-Alvarado E (2005) The effect of supercooling on crystallization of cocoa butter-vegetable oil blends. J Am Oil Chem Soc 82:471–479
14. Martini S, Herrera ML, Hartel RW (2001) Effect of cooling rate on nucleation behavior of milk fat–sunflower oil blends. J Agric Food Chem 49:3223–3229
15. Toro-Vazquez J, Herrera-Coronado V, Dibildox-Alvarado E, Charo-Alonso M, Gomez-Aldapa C (2002) Induction time of crystallization in vegetable oils, comparative measurements by differential scanning calorimetry and diffusive light scattering. J Food Sci 67: 1057–1065
16. Narine SS, Marangoni AG (1999) Relating structure of fat crystal networks to mechanical properties: a review. Food Res Int 32:227–248
17. Campos R, Narine SS et al (2002) Effect of cooling rate on the structure and mechanical properties of milk fat and lard. Food Res Int 35:971–981
18. Bouzidi L, Boodhoo M, Humphrey K, Narine S (2005) Use of first and second derivatives to accurately determine key parameters of DSC thermographs in lipid crystallization studies. Thermochim Acta 439:94–102
19. Narine SS, Humphrey KL (2004) Extending the capability of pulsed NMR instruments to measure solid fat content as a function of both time and temperature. J Am Oil Chem Soc 81:101–102
20. Tan CP, Man YBC (2002) Differential scanning calorimetric analysis of palm oil, palm oil based products and coconut oil: effects of scanning rate variation. Food Chem 76:89–102
21. Herrera M, Marquez Rocha F (1996) Effects of sucrose ester on the kinetics of polymorphic transition in hydrogenated sunflower oil. J Am Oil Chem Soc 73:321–326
22. Humphrey KL, Moquin PHL, Narine SS (2003) Phase behavior of a binary lipid shortening system: from molecules to rheology. J Am Oil Chem Soc 80:1175–1182
23. Humphrey KL, Narine SS (2004) A comparison of lipid shortening functionality as a function of molecular ensemble and shear: crystallization and melting. Food Res Int 37:11–27
24. Narine SS, Humphrey KL (2004) A comparison of lipid shortening functionality as a function of molecular ensemble and shear: microstructure, polymorphism, solid fat content and texture. Food Res Int 37:28–38
25. Marangoni A, Lencki R (1998) Ternary phase behavior of milk fat fractions. J Agric Food Chem 46:3879–3884
26. Marangoni AG, Rousseau D (1998) The influence of chemical interesterification on physicochemical properties of complex fat systems—1. Melting and crystallization. J Am Oil Chem Soc 75:1265–1271
27. Christian JW (1975) In: The theory of transformations in metals and alloys, formal theory of transformation kinetics, Pergamon, Oxford, pp. 525–548